TRENDS AND TECHNIQUES

FOR

SPACE BASE ELECTRONICS

George C. Marshall Space Flight Center
Marshall Space Flight Center, Alabama 35812

by

J.D. Trotter, P.I. J.D. Gassaway
T.E. Wade Q. Mahmood

Microelectronics Research Laboratory
Mississippi State University
Department of Electrical Engineering
Mississippi State, Mississippi 39762

QUARTERLY REPORT

March 10, 1978 - June 10, 1978

CONTRACT NAS8-26749

TRENDS AND TECHNIQUES

FOR

SPACE BASE ELECTRONICS

Prepared for

George C. Marshall Space Flight Center
Marshall Space Flight Center, Alabama 35812

by

J.D. Trotter, P.I. J.D. Gassaway
T.E. Wade Q. Mahmood

Microelectronics Research Laboratory
Mississippi State University
Department of Electrical Engineering
Mississippi State, Mississippi 39762

TECHNICAL REPORT STANDARD TITLE PAGE

1. REPORT NO.	2. GOVERNMENT ACCESSION NO.	3. RECIPIENT'S CATALOG NO.

4. TITLE AND SUBTITLE
A STUDY OF TRENDS AND TECHNIQUES FOR SPACE BASE ELECTRONICS

5. REPORT DATE
June, 1978

6. PERFORMING ORGANIZATION CODE

7. AUTHOR(S)
J.D. Trotter, J.D. Gassaway, T.E. Wade, Q. Mahmood

8. PERFORMING ORGANIZATION REPORT #
MSU-EE-QUAR-3-78

9. PERFORMING ORGANIZATION NAME AND ADDRESS
Department of Electrical Engineering
Mississippi State University
Mississippi State, MS 39762

10. WORK UNIT NO.

11. CONTRACT OR GRANT NO.
NAS8-26749

13. TYPE OF REPORT & PERIOD COVERED
QUARTERLY PROGRESS
March 10 - June 10, 1978

12. SPONSORING AGENCY NAME AND ADDRESS
National Aeronautics and Space Administration
Washington D.C. 20546

14. SPONSORING AGENCY CODE

15. SUPPLEMENTARY NOTES
Prepared by Mississippi State University for George C. Marshall Space Flight Center, Marshall Space Flight Center, Alabama

16. ABSTRACT

During the first quarter, progress was made in all three areas which were included in the scope of work. The following report describes the work done in three sections. A sputtering system was developed to deposit aluminum and aluminum alloys by the D.C. sputtering technique. This system is designed for a high level of cleanliness and for monitoring the deposition parameters during film preparation. This system is now ready for studying the deposition and annealing parameters upon double-level metal preparation. A new technique recently applied for semiconductor analysis, the finite-element method, was studied for use in the computer modeling of two-dimensional MOS transistor structures, and it was concluded that the method has not been sufficiently well developed for confident use at this time. An algorithm has been developed for implementing a computer study which is based upon the finite-difference method. The program which was developed during the last scope of work was modified and used to calculate redistribution data for boron and phosphorous which had been predeposited by ion-implantation with range and straggle conditions typical of those used at MSFC. Data was generated for <111> oriented SOS films with redistribution in N_2, dry O_2 and steam ambients. Data will be given in the final report showing both two dimensional effects and the evolution of the junction depth, sheet resistance and integrated dose with redistribution time.

17. KEY WORDS	18. DISTRIBUTION STATEMENT
2-D Diffusion SOS Diffusion Ion-implanted predeposits	

19. SECURITY CLASSIF. (of this report)	20. SECURITY CLASSIF. (of this page)	21. NO. OF PAGES	22. PRICE
Unclassified	Unclassified		

MSFC - Form 3292 (May 1969)

For sale by National Technical Information Service, Springfield, Virginia 22151

TABLE OF CONTENTS

LIST OF FIGURES

1. DOUBLE-LEVEL METALLIZATION TECHNIQUES

Most of the work during the first quarter was directed toward the development of a sputtering system for preparing aluminum and aluminum-alloy films. A photograph of the completed system is shown in Figure 1.1. Briefly, the system consists of the following.

The basic vacuum system is a Varian-NRC 6 inch oil diffusion and mechanical roughing pump equipped for automatic and manual operation. The diffusion pump is equipped for LN_2 cooling of the cold trap. The sputter gun and power supply were obtained from Sloan Technology. The sputtering chamber was designed and built at Mississippi State. It consists of a Corning 12x18 glass cylinder and an aluminum top plate machined to accomodate up to three sputter guns. A cold cathode discharge gauge was constructed and installed in the baseplate of the chamber to measure the pressure during the sputtering operation. A throttle valve with several threaded holes for accomodating plugs is operated by one of two mechanical feed-throughs in the base plate. A lift mechanism with a reversible motor was designed and contructed for raising the top plate and sputter guns.

Inside the chamber is equipped with a rotating table which accomodates up to eight wafers of 1½-2" in diameter. The table is driven by a vacuum sealed shaded pole motor through a magnetic coupling at 7 rpm. The entire motor-table assembly is rotated by a chain-sprocket-mechanical feedthrough arrangement through three sputter-gun and two mask positions. The mask is attached to the

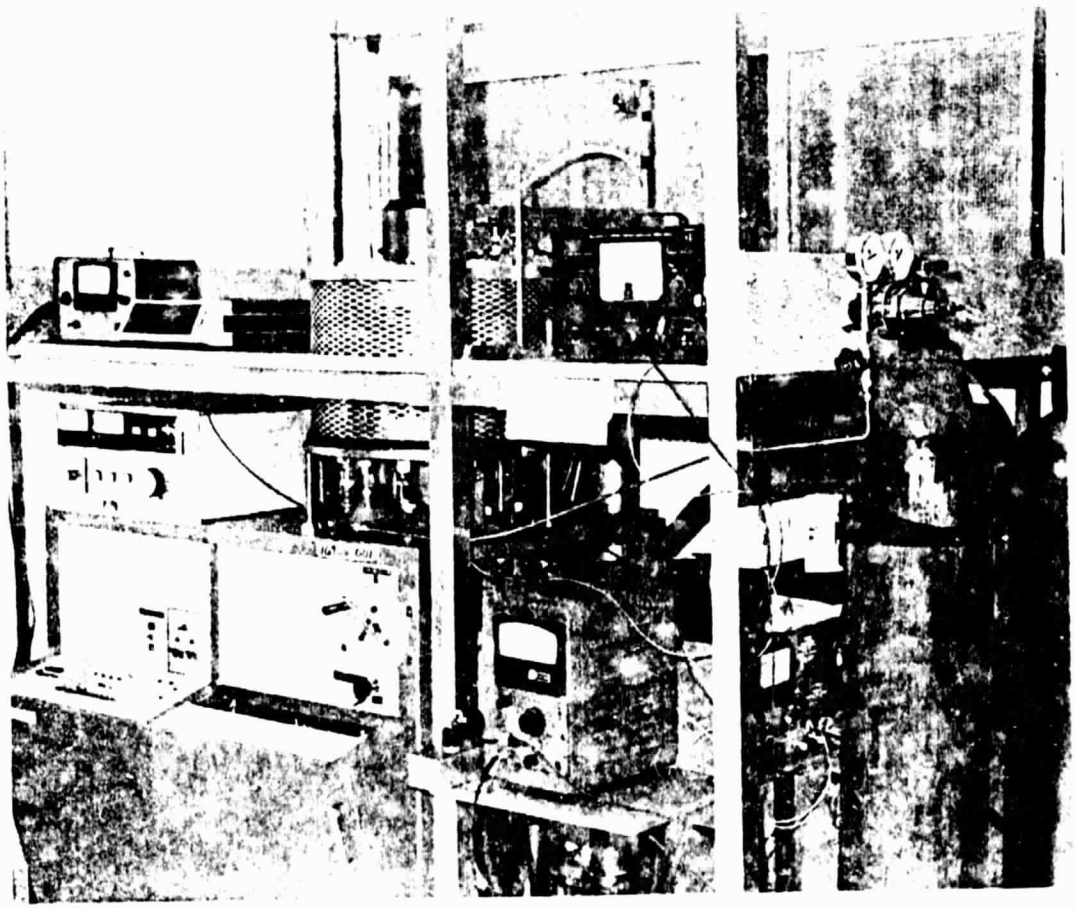

Figure 1.1 Photograph of metallization system using sputter-gun source.

rotating assembly and provides one hole through which the sputter-gun deposits metal on the wafers. A crystal film thickness sensor is located beneath the sputter-gun and receives a deposit through a hole at an unused wafer position on the table.

The sputtering chamber opens into a class 100 clean bench in order to maintain a high level of cleanliness. The system is located in the metallizing and bonding room of the microelectronics laboratories in Simrall Engineering Building, and this room was designed with air conditioning and filtering units to maintain a class 10,000 environment. The entire system has been constructed and checked out and is ready for depositing sputtered films.

The installation of a six-tube Thermco Ranger diffusion furnace was completed with the addition of a venting system for exhausting the scavenger boxes. All that remains to be done is to line the tube and connect the nitrogen ambient source in order to anneal the aluminum films.

2. TWO-DIMENSIONAL MODELS FOR MOS TRANSISTORS

The work done during the first quarter was directed toward preliminary investigations of numerical schemes and computational algorithms for solving the semiconduction equations for a two-dimensional field.

A recent report has described the application of the finite-element method to the analysis of a JFET[1]. The finite-element method has been used for some time in solving problems in mechanics and elasticity; however, it has only recently been applied to

semiconduction problems. This method has the power to treat some problems, such as eigen-value problems, for which the finite-difference method is awkward if at all applicable. It can also be applied to the solution of field distributions governed by partial differential equations, and one of the most attractive features as compared to the finite-element method is purported to be the ease of treating non-rectangular geometries and irregular boundaries. For example, the geometry of the VMOS structure could be accomodated. It was decided to further investigate this technique.

In order to better understand the applicability of the method, it was applied to a one-dimensional linear diffusion problem. This simple problem is one for which familiar results are available for comparison and at the same time taxes the finite-element method. In its most valid form, the finite element method is applicable to variational problems in which a true minimum of an energy-related function exists. Such a minimum does not apply for the semiconductor problem in which current flow occurs by diffusive and conductive mechanisms. It has been proposed that a "weak form", the so-called Galerkin method, be applied to such problems.[2] The typcial seminconductor problem is a non-linear boundary value and initial condition problem of which the linear diffusion problem is a very special case. In the example chosen, the diffusion variable, u, obeys:

$$u(x,t)\big|_{x=0} = u_s = 1 \quad (a) \qquad (2.1)$$

$$u_x(x,t)\big|_{x=a} = 0 \quad (b)$$

$$u(x,t)\big|_{t=0} = \begin{matrix} 1 \text{ , } x=0 \\ 0 \text{ , } x>0 \end{matrix} \quad (c)$$

$$u_t - u_{xx} = f(x,t) = 0 \quad 0<x<a \qquad (2.2)$$

The Galerkin formulation of this problem is:

$$\int_0^a (u_t v - u_x v_x - fv)\ dx = 0, \qquad (2.3)$$

where v(x,t) represents a "trial function" which is used to approximate u(x,t). The finite element methods uses a set of "hill functions" as illustrated in Figure 2.1 to construct the v(x,t) approximation. Two of the popular hill functions are the Hermite bicubic and the bilinear functions which are illustrated in the figure and were used in the example. The final form of the approximate solution is;

$$v(x,t) = \sum_{i=1}^{N} q_i(t)\ \phi_i(x)\ . \qquad (2.4)$$

On the node points the solution is approximated by the set $\{q_i(t)\}$ for the type of hill functions which overlap as illustrated in Figure 2.1. Solution for the set $\{q_i(t)\}$ is then analogous to solving for the set $\{u_i(t)\}$ on the node points using the finite difference technique. The equations for the set $\{q_i(t)\}$ are obtained by substituting (2.4) into (2.3).

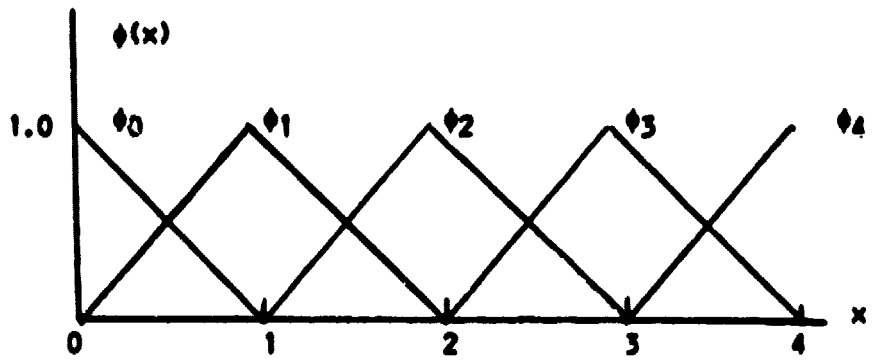

(a) Bilinear hill functions

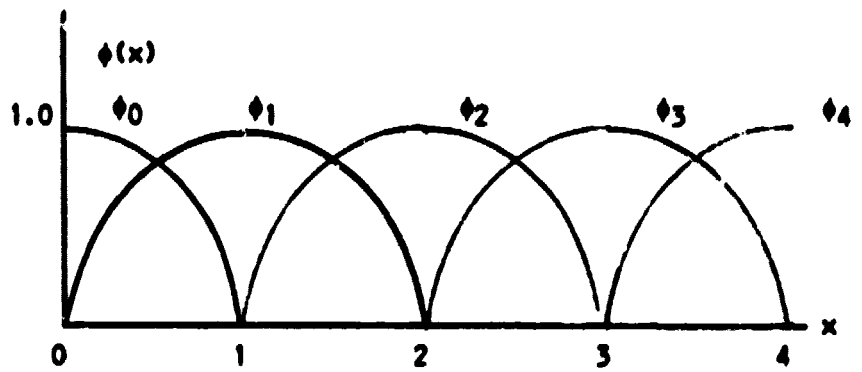

(b) Bicubic (Hermite) hill functions

Figure 2.1. Illustration of hill functions used in finite element method.

$$\sum_{i=1}^{N} \int_0^a \left(\frac{\partial q_i}{\partial t} \phi_i \phi_j + q_i \frac{\partial \phi_i}{\partial x} \frac{\partial \phi_j}{\partial x} + f_j \right) dx = 0$$

$$j = 1,2,3,.....N \qquad (2.5)$$

From (2.5) a set of time differential equations is obtained which is solved using an implicit numerical method.

The solution of the problem posed by the example is closely approximated by the erfc function in the range $0 \leq x \leq 3$ if $a = 6$, and this solution was used to compare the accuracy of the finite element and finite difference methods. Figures 2.2-2.4 show the maximum error as a function of the reciprocal of the number of grid points and the size of the time step, i.e. $\lambda^2 = \Delta t/\Delta x^2$.

The error obtained in the solution by the bilinear finite element method is very nearly the same as that obtained with the finite difference method. This was not surprising because the system of equations for $\{q_i(t)\}$ and $\{u_i(t)\}$ were quite similar. What was surprising was that the Hermite bicubic finite element produced such poor results, although this surprise was based upon the intuition that since this element was more difficult to use it should provide some reward for the difficulty.

This experience resulted in some skepticism that the finite element method would be effective for semiconductor problems. A more recent paper has reinforced this attitude.[3] This paper indicates that the proper formulations of the semiconductor problem

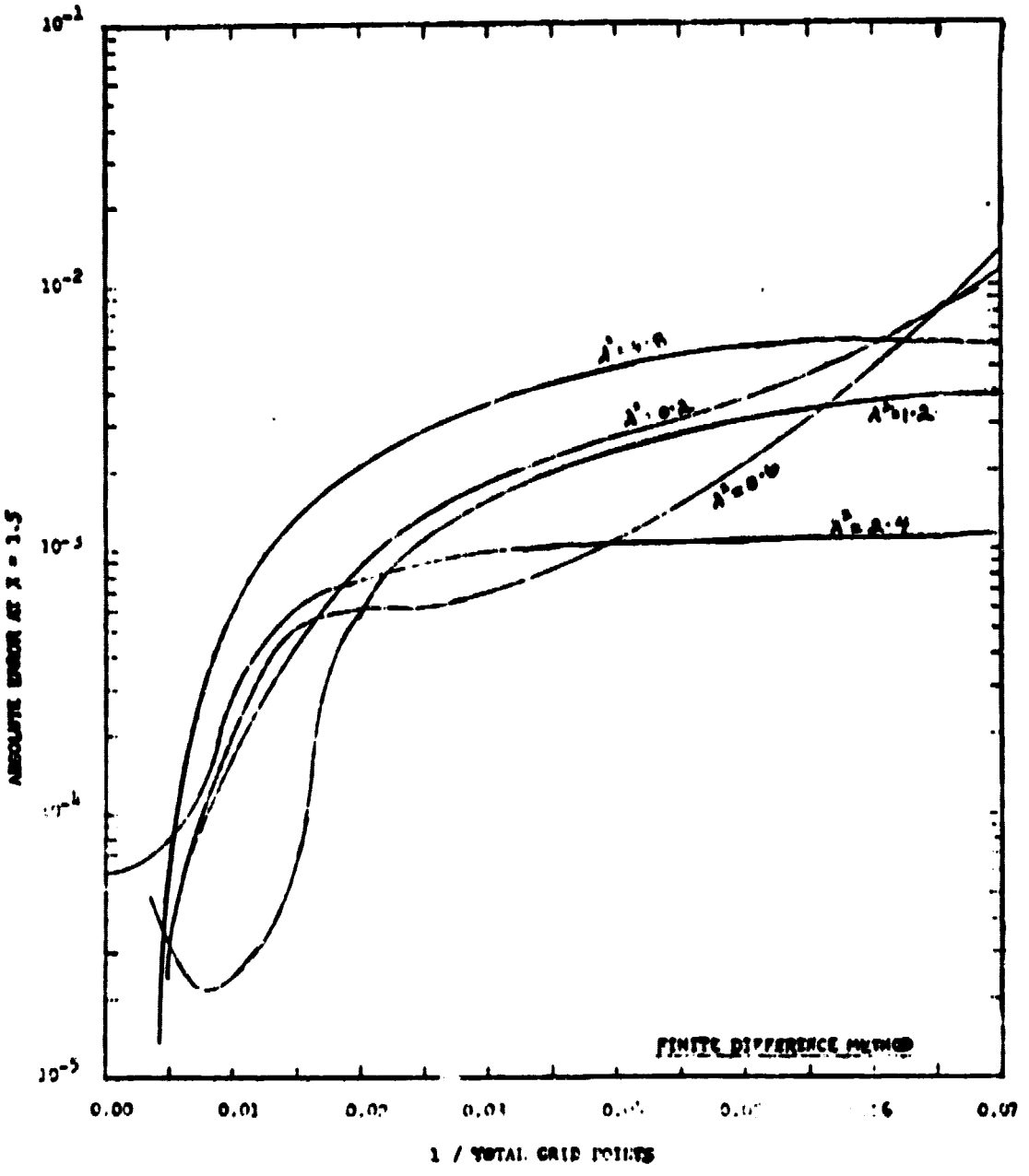

Figure 2.2. Error for finite-difference vs. reciprocal of total number of grid points.

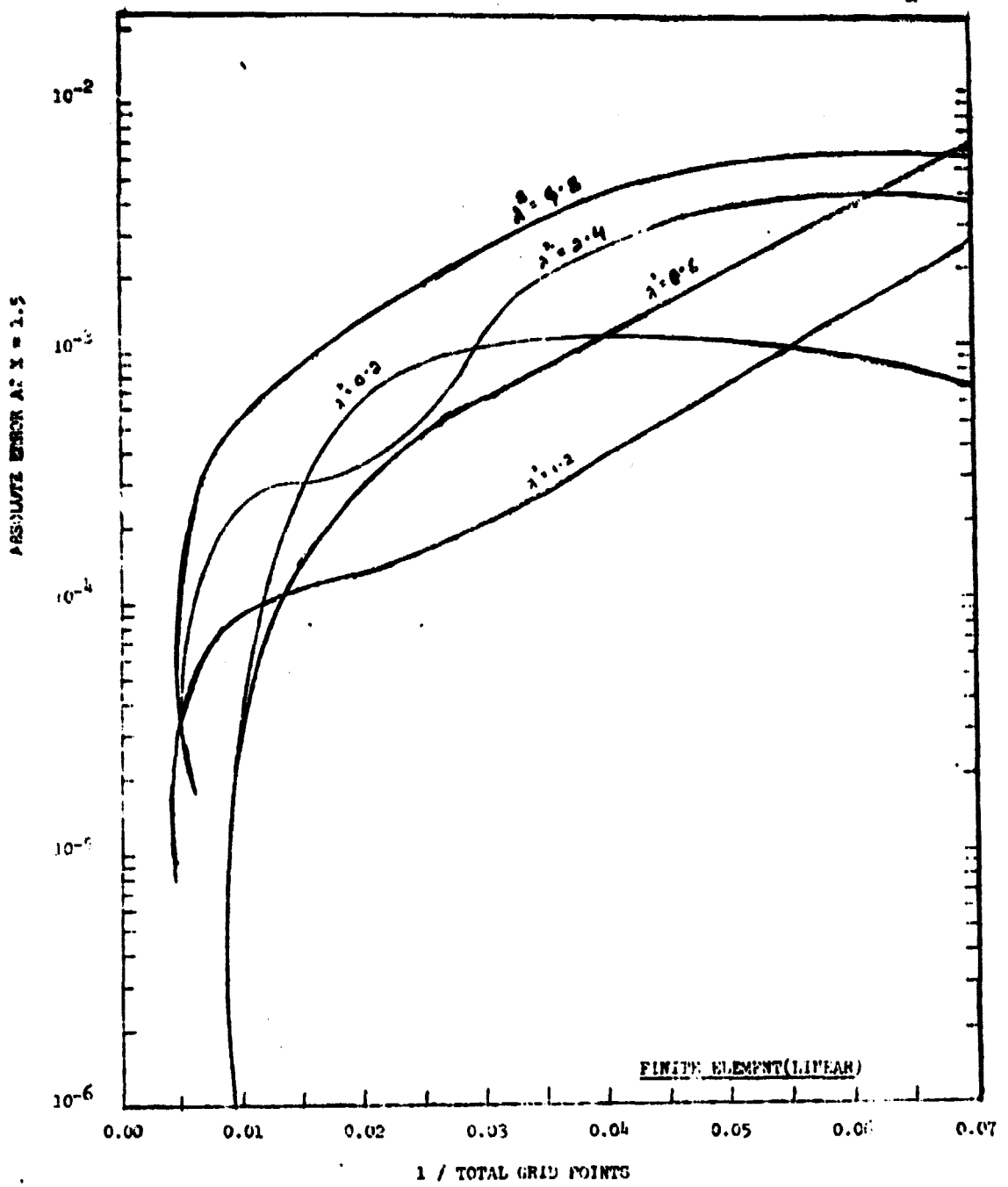

Figure 2.3 **Error for finite-bilinear element vs. reciprocal of total number of grid points.**

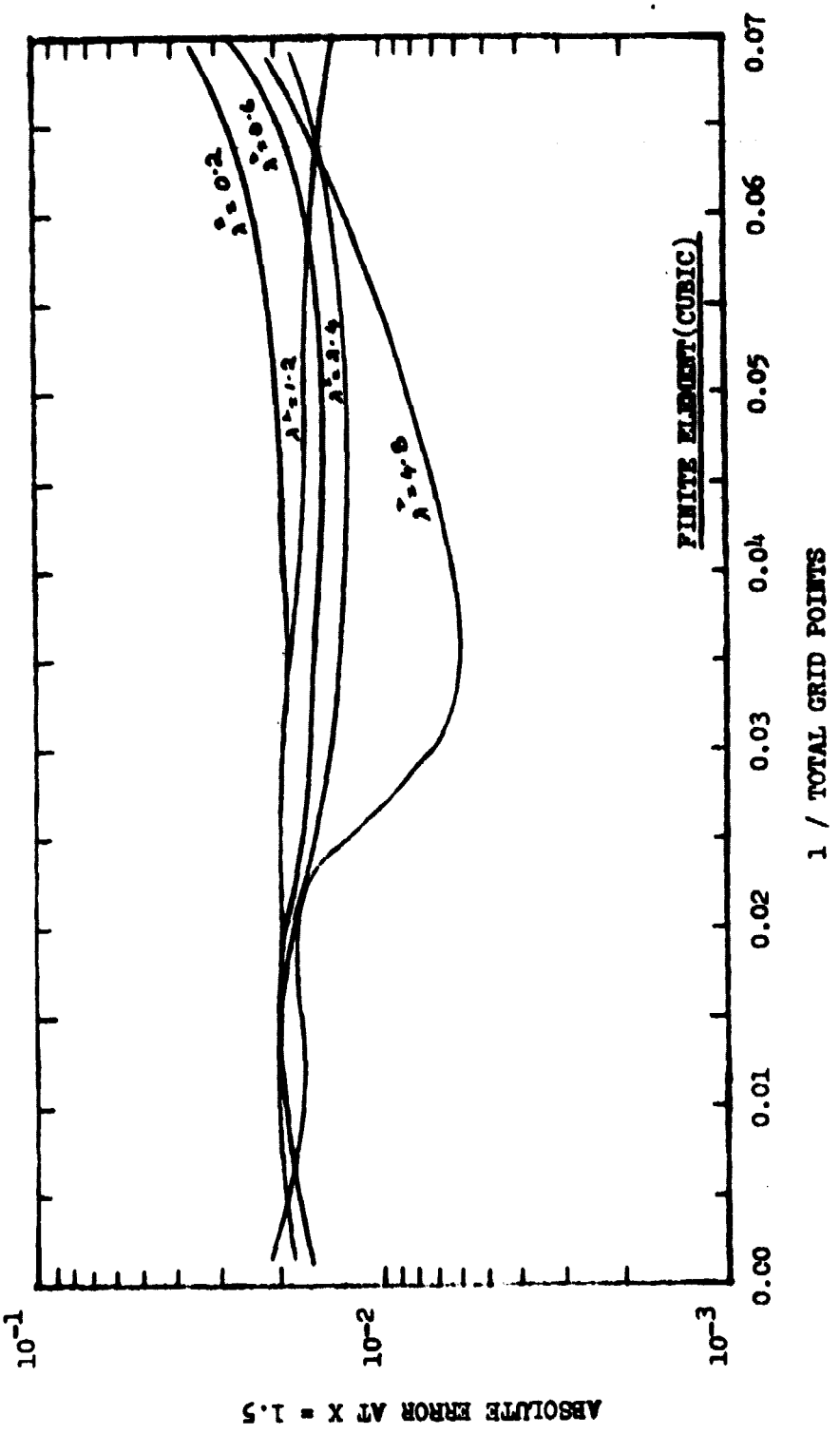

Figure 2 4 Error for finite-bicubic-element vs. reciprocal of total number of grid points.

for the finite element approach remain to be demonstrated, and, in agreement with our observations, point out that the application of Galerkin's method is subject to skepticism. Therefore, it was concluded that the further work should be based upon the finite-difference method which we have used before although the finite-element method is intriguing and may be further developed in the future.

The second phase of this program is underway to develop a computational program with which to generate data from a model. During the past quarter, the major emphasis was upon deriving a simple two-dimensional algorithm which could be economically used in a simulation program during its development. It is plausible that this algorithm can be later modified to become adequate for modeling of other effects which are significant in certain situations, e.g., short channel effects, avalance breakdown, etc.

During the past quarter an algorithm has been developed based upon the usual assumption that the mobile carriers are included in an infinitesimally thick layer of charge at the $Si-SiO_2$ interface. The current flow is then described by a one-dimensional equation:

$$i = \frac{kT}{q} \mu_N \left(\frac{\partial \mu}{\partial X} L \ S + \frac{q\mu}{kT} L \ E_s S \right) , \ 0 \leq x \leq a \qquad (2.6)$$

where i and S are channel current and charge per unit channel width, E_s is the tangential interface field and μ_N and μ_L are the mobility factors accounting respectively for gate modulation and hot electron effects. This equation is solved iteratively with

Poisson's equation which includes two dimensional effects:

$$\nabla^2\psi = -\rho/\epsilon \quad . \tag{2.7}$$

Equation (2.7) will be solved for one segment of a periodic structure with respect to x and equation (2.6) will be integrated to produce auxiliary equations for the boundary conditions at the $Si-SiO_2$ interface. It will be assumed initially that $S = 0$ at $x = a$, the point at which the normal component of the interface field changes sign. The solution algorithm then proceeds in an iterative fashion to solve (2.6) and (2.7) simultaneously for the potential distribution from which the current, i, is untimately calculated as a function of the gate, drain and body voltage.

The model at this point admittedly has some short-coming, mainly due to the neglection of generation-recombination mechanisms. Therefore, it will not treat impact avalance and bulk generated leakage currents. It is believed at this time that such effects can be treated by adding another iterative loop to the algorithm. The major emphasis at this point will be the development of a program for input and output data management and including subroutines which generate data internally within the program and solve systems of equations which will be encountered in implementing the algorithm.

3. REDISTRIBUTION DIFFUSIONS FOR ION-IMPLANTED PREDEPOSITS OF BORON AND PHOSPHORUS IN SOS FILMS.

The objective of this work was to produce curves describing the variation with diffusion time and temperature of the junction depth, sheet resistance and integrated impurity dose. This data has been generated for boron and phosphorus redistributed in nitrogen, dry oxygen and steam ambients for <111> oriented SOS films. The following section presents discussions of the implantation and redistribution model, further program develop, the computational procedure and of the computed results.

3.1 The Redistribution Model:

There are three aspects of the redistribution model which are considered: (a) the implanted profile, (b) the oxidation model, and (c) the diffusivity model.

(a) The implanted profile. The implanted profile is described by the gaussian function,

$$C(y) = C_{max} \exp\left\{-\tfrac{1}{2}\left(\frac{y - R_p}{\Delta R_p}\right)^2\right\}, \qquad (3.1)$$

where C is the concentration, y is the distance from the entrant silicon surface, R_p is the range and ΔR_p is the straggle for the implant. The peak concentration, C_{max}, is related to the implant dose, Q_{imp} by:

$$C_{max} = Q_{imp} / \sqrt{2\pi}\, \Delta R_p \ . \qquad (3.2)$$

Redistribution data has been generated for the following conditions:[4]

Q_{imp}:	$5x10^{12}$, 10^{13} , $5x10^{13}$, 10^{14} cm^{-2}	
R_p:	0.2735 μm	80 keV boron implant.
	0.1727 "	150 keV phosphorus.
ΔR_p:	0.0665 μm	80 keV boron implant.
	0.0440 "	150 keV phosphorus.

The doses are light to moderate resulting in concentrations no heavier than $6x10^{18}$ cm^{-3}, and the range-straggle values are typical of those employed at MSFC. It is assumed that all of the ions become activated shortly after redistribution begins and thereby diffuse by a substitutional mechanism involving vacancies.

(b) Oxidation Model: The oxidation model is assumed to be the same as for bulk silicon and the data of Deal et.al.[5] has been used to calculate the oxidation rate according to:

$$\frac{dx_o}{dt} = B/(2x_o + B/C) , \qquad (3.3)$$

where B and C follow Boltzmann-like temperature dependences. Figures (3.1) and (3.2) illustrate the oxide thickness dependence upon time and temperature for both dry O_2 and steam ambients.

During the oxidation, the silicon film thickness is reduced according to:

$$W = W_o - \alpha x_o , \qquad (3.4)$$

where W_o is the initial film thickness, taken to be 1 μm, and $\alpha = 0.45$ is the ratio of the densities of SiO_2 to silicon.

Redistribution data is given for W_o = 1 μm and an initial oxide thickness of x_o = 300 Å.

(c) Diffusivity Model: The diffusivity model for boron was discussed in an earlier report[6] and it includes a linear dependence of the diffusivity upon the vacancy concentration as well as the field-enhancement effect. The diffusivity model for phosphorus includes only the field-enhancement effect which is sufficient to describe the non-linear behavior of phosphorus diffusions at concentrations lower than 10^{19} cm^{-3} as shown by Barry [7] and Fair and Tsai[8]. The diffusivity-temperature dependence is after Fair[9] and Fair and Tsai[8] adaptation of data by Ghostagore[10]. For either boron or phosphorous the effective diffusivity is given by:

$$D_{eff} = D(u) \times (1 + u/\sqrt{u^2 \pm 1}) \quad , \tag{3.4}$$

where,

$$u = C/ 2 n_i, \tag{3.5}$$

and,

$$D(u) = D_B^* u \text{ , for boron,} \tag{3.6}$$

$$= D_p^* \text{ , for phosphorus.}$$

and where n_i is the intrinsic carrier concentration at the diffusion temperature and D_B^* and D_p^* are the intrinsic diffusivities of boron and phosphorus:

$$D_B^* = 3.17 \exp (-3.59eV/ k_BT) \ cm^2/sec.,$$

$$D_p^* = 3.85 \exp (-3.66eV/ k_BT) \tag{3.7}$$

3.2 Further Program Development

The program which was used to generate the data has been described in detail in an earlier report. It was noted that the program was developed in such a way that one could take advantage of a normalization procedure for predeposition diffusions and generate data applicable to different film thicknesses. However, it is not possible to gain such an advantage for redistribution diffusions involving ion-implants or growth of an oxide. Then the program was used to generate data, it was discovered that some other features of the program are extraneous unless further refined.

The program was developed to account for both thin and thick oxides such as would be encountered in some practical situations. However, such a simulation requires the incorporation of a warped grid system, a modification which would require considerably more effort. Therefore, the variable oxide feature is of limited value at this time, since the program, at best, only approximates the conditions for growth of a very thin oxide during redistribution.

A modification was made which allows accurate treatment of redistribution under oxidizing conditions when only a single oxide thickness is involed. The original program treated the oxidation process with regard to the boundary conditions; however, unlike the case of bulk silicon, one must also account for the reduction of the silicon film thickness. This feature is now included in the program. During the simulation of a redistribution in an oxidizing ambient, the vertical grid spacing continuously shrinks

while the horizontal grid spacing is constant. The modification does not show up on logic flow diagrams at the level of detail which has previously been given. For completeness, a new listing of the affected main and sub-programs will be given in the Final Report.

3.3 Computational Procedure;

The program described in an earlier report, and modified as described in the preceding, was used to generate the data. Two-dimensional data was obtained in the form of isoconcentration contours for typical situations. The bulk of the data which can be correlated with experimental measurements is generated using a quasi-one-dimensional model in a manner described in a previous report[6]. A brief review of the procedure is given in the following.

For generation of sheet resistance, junction depth and integrated impurity dose data as a function of time and temperature, only a one-dimensional profile need be calculated. This is accomplished by making the horizontal grid only three units wide but keeping the field six film thicknesses wide. Periodic boundary conditions for the horizontal dimensions are employed in the program and result in a calculation which produces the vertical profile equivalent to a none-dimensional model. Thus without sacrificing the generality of the program for treating two-dimensional cases, the amount of computing time is drastically reduced when the data that is desired does not require the full power of the program.

The vertical grid varies from thirty one to sixty one points as required for accuracy in details of the profile, and most of the data is not sensitive to the number of grid points used if the number is chosen in this range. For the purpose of illustrating the unusual nature of phosphorous profiles, the larger number of points was required.

3.4 Discussion of Results

First, some of the unusual behavior of redistribution diffusions in SOS films will be discussed in this section. Next, the format for the calculated curves will be discussed.

Figures (3.1) and (3.2) illustrate the oxide thickness growth and silicon film thickness reduction as functions of time for <111> silicon silms oxidized in steam and dry O_2 ambients. The evolution traced beginning with an initial oxide of 300 Å thickness on an SOS film of 1 μm initial thickness. The curves are shown for four temperatures. The data are necessary for interpreting some of the results for simulated redistributions.

Figures (3.3) and (3.4) show impurity profiles for boron and phosphorus implants being redistributed in a steam ambient at 1000 deg. C. The profiles are all plotted with a common origin as would be the case for experimentally derived profiles where Si-SiO_2 interface would serve as the logical origin. However, the profiles are normalized with respect to the film thickness which is of course shrinking. The boron profiles are not unusual but show the wellknown leaching effect due to segregation into

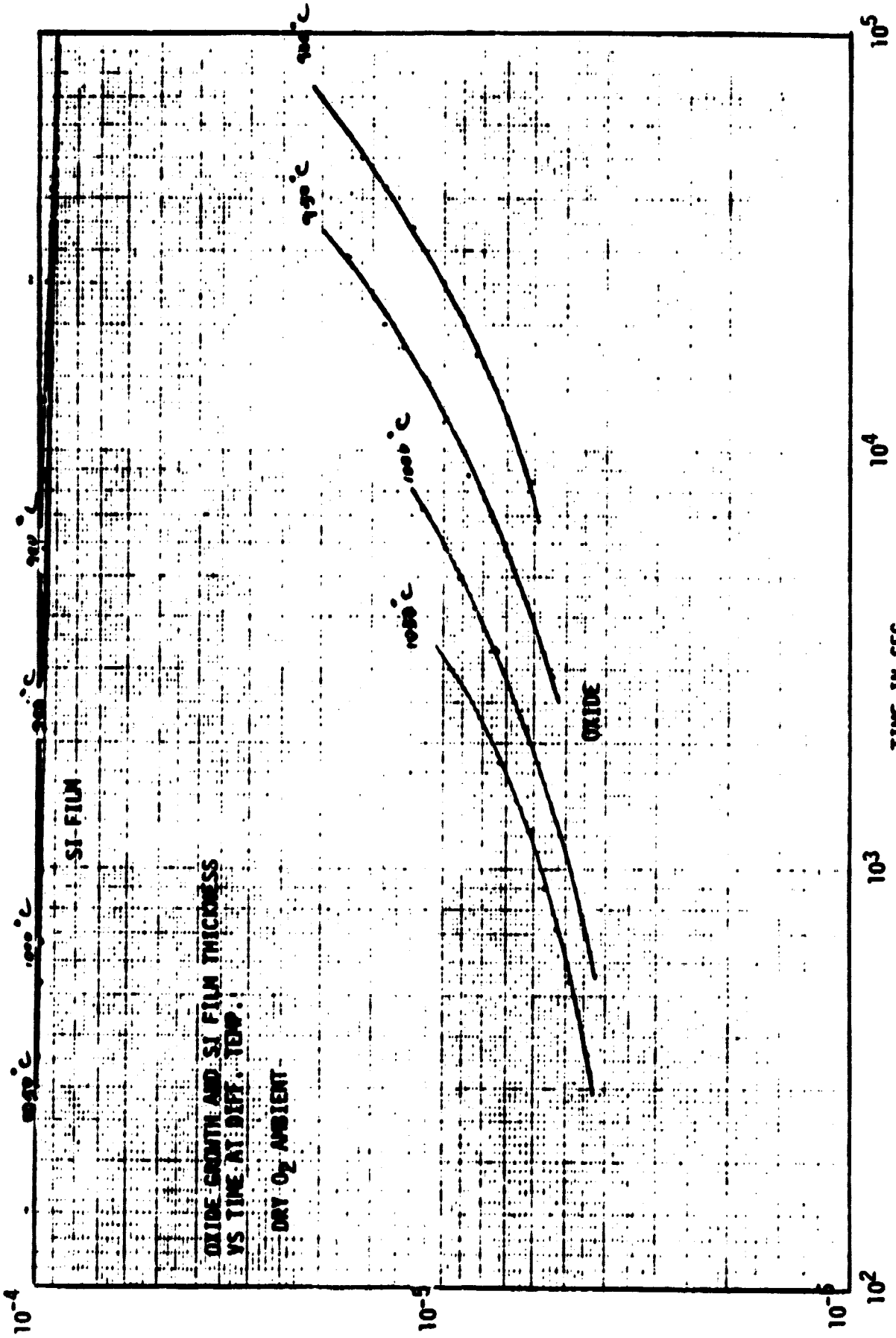

Figure 3.1

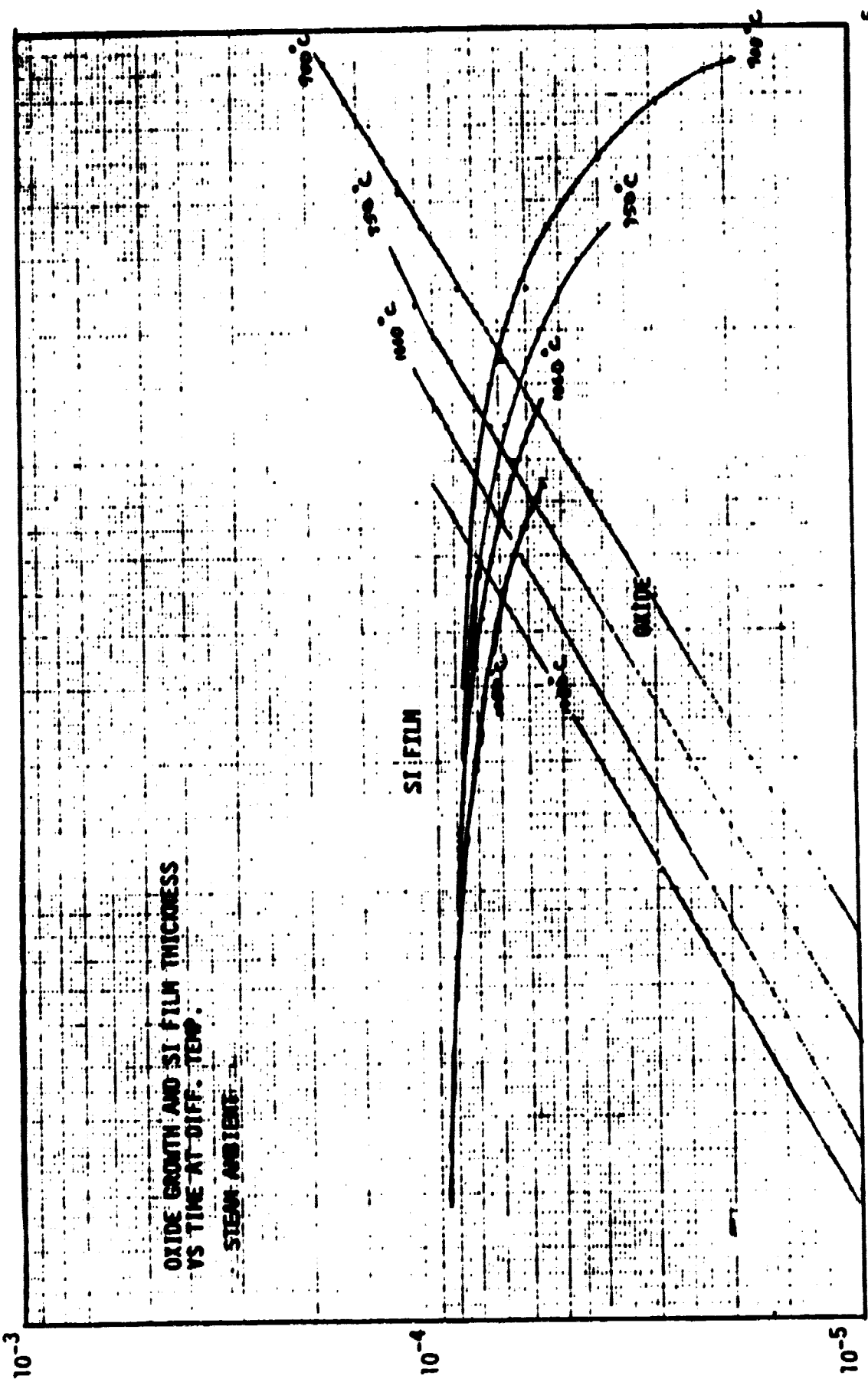
OXIDE GROWTH AND SI FILM THICKNESS
VS TIME AT DIFF. TEMP.
STEAM AMBIENT
SI FILM
OXIDE
THICKNESS IN CM.
TIME IN SEC
10^{-3}
10^{-4}
10^{-5}
10^{2}
10^{3}
10^{4}
10^{5}

Figure 3.2

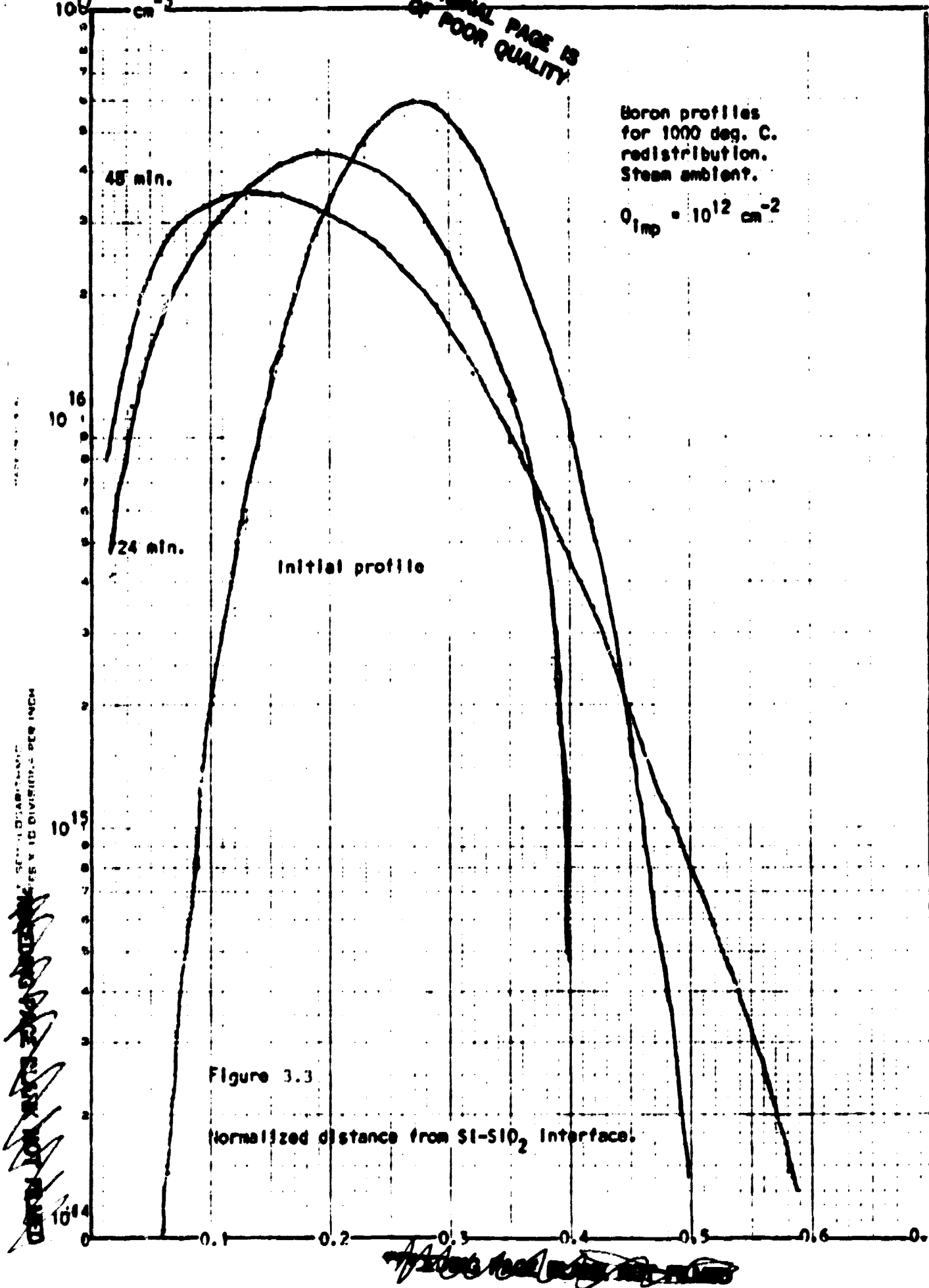

Figure 3.3

Normalized distance from Si-SiO_2 interface.

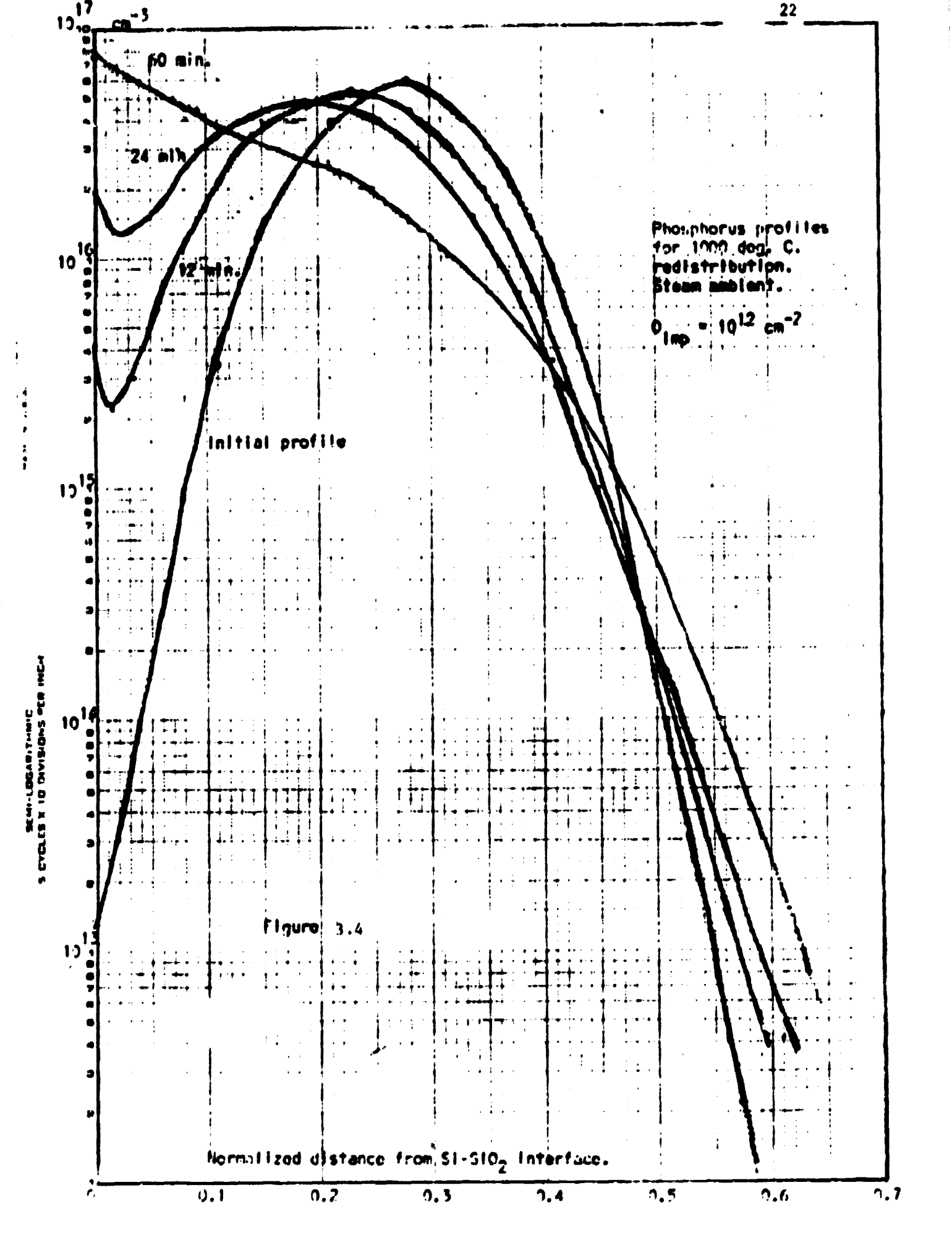
10^{17} cm^{-3}
10^{16}
10^{15}
10^{14}
10^{13}
60 min.
24 min.
12 min.
Initial profile
Phosphorus profiles for 1000 deg. C. redistribution. Steam ambient.
$Q_{imp} = 10^{12}$ cm^{-2}
SEMI-LOGARITHMIC 5 CYCLES X 10 DIVISIONS PER INCH
Normalized distance from Si-SiO$_2$ interface.
0
0.1
0.2
0.3
0.4
0.5
0.6
0.7

Figure 3.4

the oxide. The phosphorus profiles show the effect of impurities being rejected from the oxide. There is a pile-up of impurities in front of the advancing Si-SiO_2 interface and then a dip which eventually disappears. It is easy for one to draw an erroneous conclusion from observing the profiles, because it appears that the integrated dose should increase or at least remain constant and the sheet resistance should decrease with time. This is not true. Although the segregation coefficient favors phosphorus in silicon vs. SiO_2, eventually all of the phosphorus will be in the SiO_2 when the SOS film is completely oxidized since the model assumes that there is no diffusion into the sapphire.

Figures (3.5-3.7) illustrate the behavior of the junction migration, sheet resistance variation, and integrated impurity dose variation over a long period of time. All of the curves are plotted with respect to normalized time, and true time is obtained by multiplying by the normalizing time value given on the plot. Junction depths are in microns, sheet resistance values are in ohms, and dose values are in cm^{-2} units unless otherwise marked. The curves are given in the typical format for all of the data.

For an ion-implanted profile, there are in fact two junctions until one of the junctions emerges at the Si-SiO_2 interface. Therefore, the sheet resistance values are for the buried layer until the front junction disappears. This typically occurs in a short time compared with that for through-diffusion of the back junction. Figure (3.5) illustrates the through-diffusion of the back junction for the heavier doses. This always occurs for redistribution in

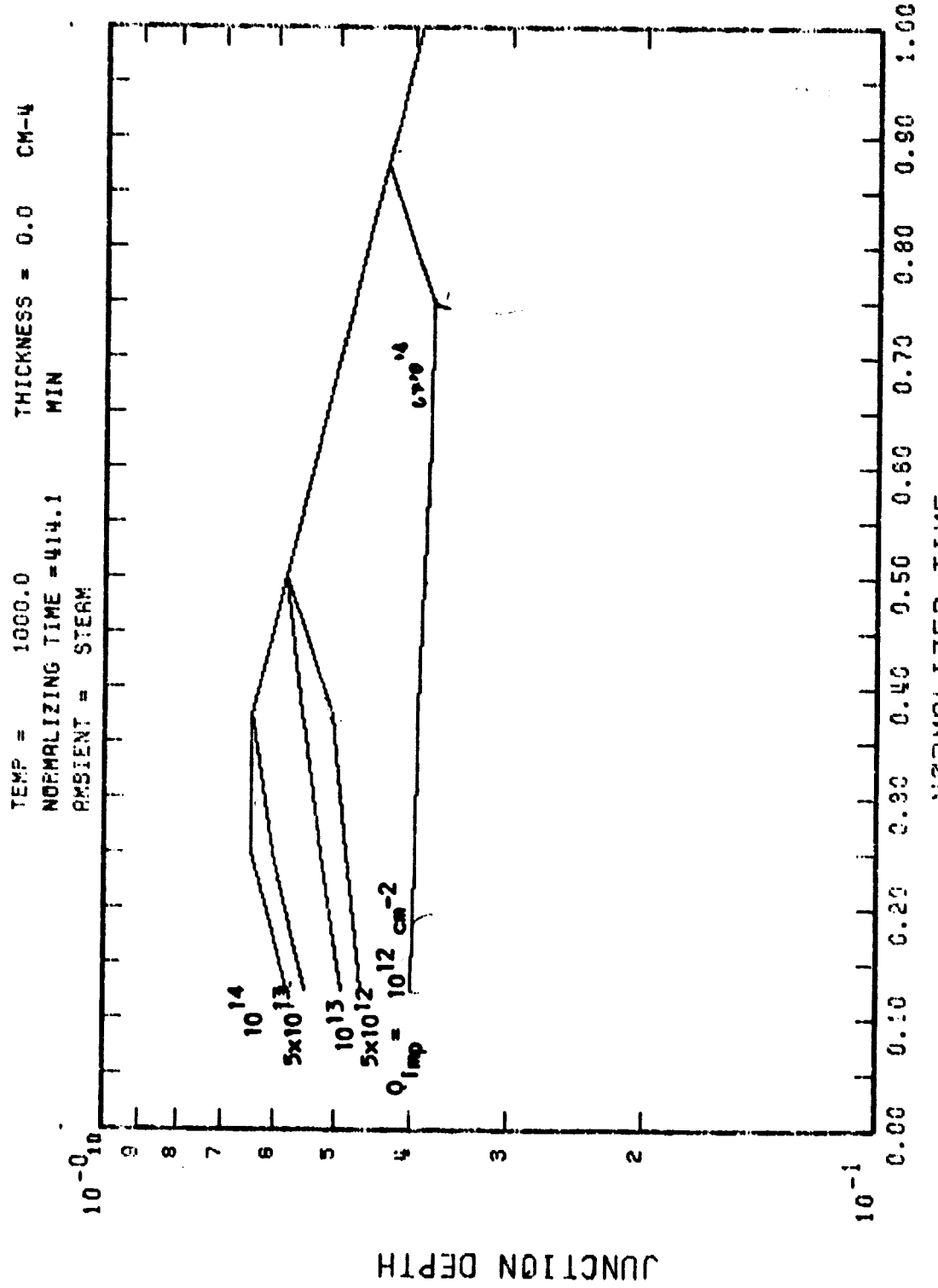

Figure 3.5 Junction position with respect to Si-SiO_2 interface for Boron redistribution.

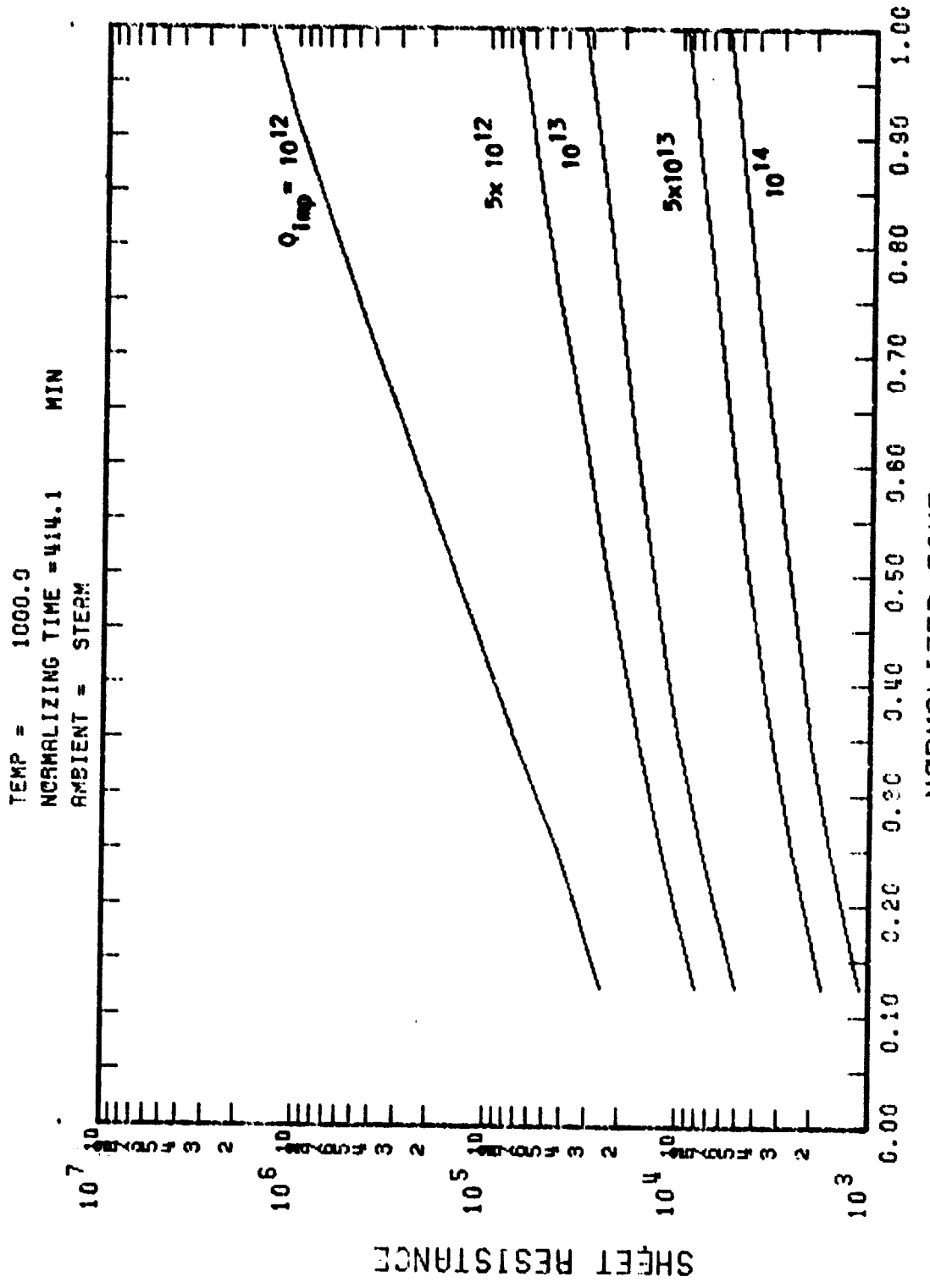

Figure 3.6 Sheet resistance for Boron redistribution.

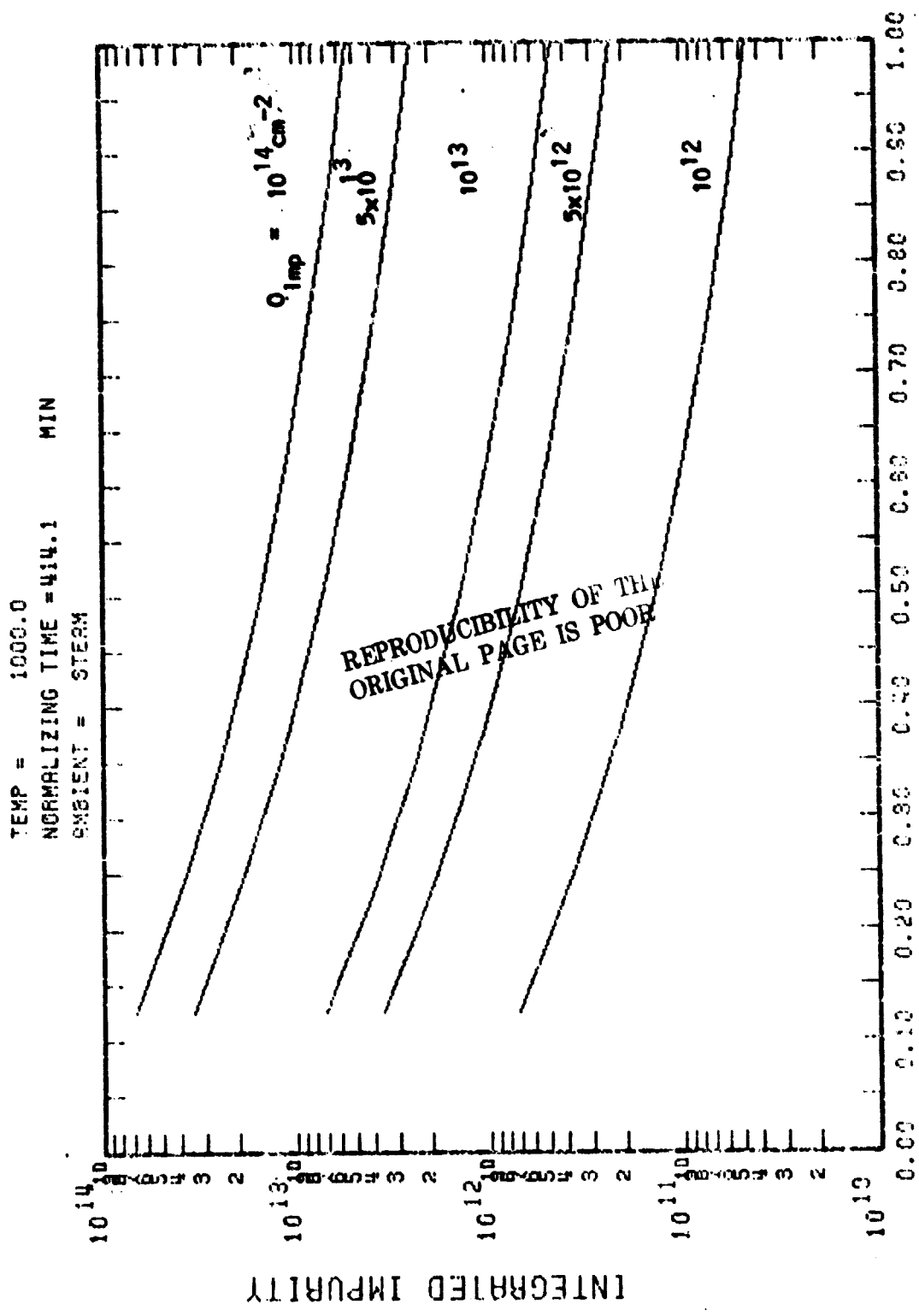

Figure 3.7 Variation of Dose for Boron redistribution.

a nitrogen ambient but not necessarily so for an oxidizing ambient. After the through diffusion, or even before for light doses, the junction depth will eventually decrease due to the reduction of the film thickness or due to the relatively slow advancement of the junction with respect to the moving Si-SiO_2 interface.

REFERENCES

1. J.J. Barnes, A Two-Dimensional Simulation of MESFETS, Technical Report, RADC-TR-76-153, May 1976.

2. G. Strang and G.L. Fix, An Analysis of the Finite Element Method, Prentice-Hall, 1973.

3. J.H. Hohl, "Variational Principles for Semiconductor Device Modeling with Finite Elements," IBM J. Res. Develop., Vol.22, No. 2, March 1978, p. 159.

4. D. Wood, Private communication p-ovided the range-straggle data.

5. B.E. Deal and A.S. Grove, "General Relationship for the Thermal Oxidation of Silicon," J. Appl. Physics, Vol. 36, No. 12, Dec. 1965, p. 3770, Deal, Sklar, Grove and Snow, "Characteristics of the Surface-State Charge of Thermally Oxidized Silicon," J. Electrochem. Soc., Vol. 114, No. 3, Mar. 1967, p. 266.

6. J.D. Gassaway and Q. Mahmood, Computer Simulation of Two-Dimensional Impurity Diffusion in Silicon-on-Sapphire Films, Interim report, NASA Contract NAS8-26749, March 1978.

7. M.L. Barry, "Doped Oxides as Diffusion Sources," J. Electrochem. Soc., Vol. 117, No. 11, Nov. 1970, p. 1405.

8. R.B. Fair and J.C.C. Tsai, "A Quantitative Model for the Diffusion of Phosphorus in Silicon and the Emitter Dip Effect," J. of Electrochem. Soc., Vol. 124, No. 7, July 1977, p. 1107.

9. R.B. Fair, "Boron Diffusion in Silicon-Concentration and Orientation Dependence, Background Effects, and Profile Estimation," J. Electrochem. Soc., Vol. 122, No. 6, June 1975, p. 800.

QUARTERLY

FINANCIAL REPORT

FOR

NASA Contract NAS8-26749

March 11, 1978 - May 31, 1978

Prepared for

George C. Marshall Space Flight Center

Marshall Space Flight Center
Alabama 35812

Submitted By

J. D. Trotter, Principal Investigator
T. E. Wade
J. D. Gassaway

COST ANALYSIS OF RESEARCH PROJECTS

CONTRACT 20-45-0210607-232 PROJECT TITLE NASA Contract NAS8-26749

DATE THIS REPORT March 31, 1978 THROUGH March 31, 1978

	EXPENDITURES THIS MONTH	EXPENDITURES TO DATE	OUTSTANDING COMMITMENTS	FREE BALANCE	TOTAL PROPOSED BUDGET
A. PERSONNEL SERVICES (1) Professional					$22,806
(2) Graduate Assistants					8,550
(3) Undergraduate Assistants					1,680
(4) Technical					
(5) TOTAL PERSONNEL SERVICES	1,318.00	1,318.00		31,718.00	33,036
B. MATERIALS AND SUPPLIES	245.92	245.92		2,604.08	2,850
C. EQUIPMENT					
D. TRAVEL	42.00	42.00		2,511.00	2,553
E. EMPLOYEE BENEFITS				3,695.00	3,695
F. OTHER (Specify) Computer Service				3,000.00	3,000
Communications	10.75	10.75		- 10.75	
G. TOTAL DIRECT EXPENDITURES					45,134
H. INDIRECT COST 45.0% of A(5)	593.10	593.10		14,272.90	14,866
I. TOTAL EXPENDITURES	2,209.77	2,209.77		57,790.23	$60,000

COST ANALYSIS OF RESEARCH PROJECTS

CONTRACT 30-45-0210607-232 PROJECT TITLE NASA Contract NASS-26749

DATE THIS REPORT April 1. 1978 THROUGH April 30, 19 78

	EXPENDITURES THIS MONTH	EXPENDITURES TO DATE	OUTSTANDING COMMITMENTS	FREE BALANCE	TOTAL PROPOSED BUDGET
A. PERSONNEL SERVICES (1) Professional					$22,806
(2) Graduate Assistants					8,550
(3) Undergraduate Assistants					1,680
(4) Technical					
(5) TOTAL PERSONNEL SERVICES	1,584.00	2,902.00		30,134.00	33.036
B. MATERIALS AND SUPPLIES	5.97	251.89		2,598.11	2,850
C. EQUIPMENT					
D. TRAVEL	19.00	61.00		2,492.00	2,553
E. EMPLOYEE BENEFITS	334.98	334.98		3,360.02	3,695
F. OTHER (Specify) Computer Service				3,000.00	3,000
COMMUNICATIONS	80.00	90.75		- 90.75	
G. TOTAL DIRECT EXPENDITURES					45,134
H. INDIRECT COST 45.0% of A(5)		593.10		14,272.90	14,866
I. TOTAL EXPENDITURES	2,023.95	4,233.72		55,766.28	$60,000

COST ANALYSIS OF RESEARCH PROJECTS

CONTRACT 30-45-0210607-232 PROJECT TITLE NASA Contract NAS8-26749

DATE THIS REPORT May 1, 1978 THROUGH May 31 1978

	EXPENDITURES THIS MONTH	EXPENDITURES TO DATE	OUTSTANDING COMMITMENTS	FREE BALANCE	TOTAL PROPOSED BUDGET
A. PERSONNEL SERVICES (1) Professional					$22,806
(2) Graduate Assistants					8,550
(3) Undergraduate Assistants					1,680
(4) Technical					
(5) TOTAL PERSONNEL SERVICES	1,559.20	4,461.20		28,574.80	33,036
B. MATERIALS AND SUPPLIES	209.30	461.19		2,388.81	2,850
C. EQUIPMENT					
D. TRAVEL	62.44	123.44		2,429.56	2,553
E. EMPLOYEE BENEFITS	51.90	386.88		3,308.12	3,695
F. OTHER (Specify) Computer Service				3,000.00	3,000
COMMUNICATIONS		90.75		- 90.75	
G. TOTAL DIRECT EXPENDITURES					45,134
H. INDIRECT COST 45.0% of A(5)		593.10		14,272.90	14,866
I. TOTAL EXPENDITURES	1,882.84	6,116.56		53,883.44	60,000